Modelling of the internal ballistics of mortar including polydisperse gunpowder size

Matthias Pautard, Christian Chauveau, Fabien Halter, Christophe Coulouarn

MODELLING OF THE INTERNAL BALLISTICS OF MORTAR INCLUDING POLYDISPERSE GUNPOWDER SIZE

Matthias Pautard[1], Christian Chauveau[2], Fabien Halter[2], and Christophe Coulouarn[1]

[1]Thales LAS France, Route d'Ardon, La Ferté-Saint-Aubin 45240, France
[2]CNRS ICARE, Avenue de la Recherche Scientifique, Orléans Cedex 2 45071, France

The propulsion of mortar ammunition has given rise to few establishments of specific simulation models [1, 2, 3] due to the reasonable costs of the experimental methods. However, the optimization of propellant architecture requires theoretical studies to better understand the phenomena involved in the propulsion phases of the projectiles into the barrel. The accessibility of simulation assets has increased in recent years, allowing fields such as interior ballistics to benefit. To deepen the theoretical knowledge of the internal ballistics of mortars by relying on advanced digital means is thus the objective of this present work.
The objective of this study is to improve the understanding of the physico-chemical phenomena that take place during the propulsion phases of mortar shells. It is therefore desirable to set up theoretical, experimental and numerical studies. This work is carried out as a collaborative effort between Thales and ICARE laboratory in order to enhance our understanding on the common fields of interest. These activities concern two-phase simulations as well as the combustion of solid energetic materials, all subjects currently under study.
The first step was to create a 0D code based on the literature. The specificity of a mortar's internal ballistics model is mostly the consideration of two chambers interacting with a compressible flow. Due to the inertia of the gun powder, this flow will induce erosive combustion [4, 5]. Another particularity of the mortar is the necessity to use a fine gunpowder, implying difficulties to produce similar sized grains in terms of dimension. Indeed, the dispersion of the grains thickness produced in series can reach 10% up to 20%, thus impacting the interior ballistics. To take this phenomenon into account, it is necessary to modify the calculation of the surface and volume according to the Population Balance Equation [6, 7].
In order to test the validity of our model while considering the high repeatability of the initial velocity of our mortar ammunition, a quick glance was given to the intermediate ballistic phase [8] to estimate the velocity gain during this step. Therefore we can better link the speed of the ammunition resulting from our code to some future measurement.
This presentation will describe current work and future prospects for applications to ballistics interior simulation of mortar.

1 INTRODUCTION

The propulsion of mortar ammunition has given rise to few establishments of specific simulation models [1, 2, 3] due to the reasonable costs of the experimental methods. However, the optimization of propellant architecture requires theoretical studies to better understand the phenomena involved in the propulsion phases of the projectiles into the barrel. The accessibility of simulation assets has increased in recent years, allowing fields such as

interior ballistics to benefit. To deepen the theoretical knowledge of the internal ballistics of mortars by relying on advanced digital means is thus the objective of this present work.
The objective of this study is to improve the understanding of the physico-chemical phenomena that take place during the propulsion phases of mortar shells. It is therefore desirable to set up theoretical, experimental and numerical studies. This work is carried out as a collaborative effort between Thales and ICARE laboratory in order to enhance our understanding on the common fields of interest. These activities concern two-phase simulations as well as the combustion of solid energetic materials, all subjects currently under study.

2 MORTAR MODELING

There are several approaches to interior ballistics that are easier than 2D or 3D models to make quick assessments, especially 1D models[9, 10, 3].
Regarding the specific case of the mortar, one can find some works, in 2D [1] or in 0D [2].
First, a code named SBIM based on a 0D model was developed as an engineering tool. This will be used to make simple calculations to test new theories in order to have preliminary information in a reasonable time. Then an additional work have been performed to implement some missing elements to the MOBIDIC code [11] in its 2D configuration in order to take into account the specificities of the mortar. This article will not go into details about MOBIDIC models which are already referenced in the literature. Erosive combustion and grain dispersion was added which will be explained here. We will therefore focus on the 0D model.
The foundation of the 0D model is the consideration of two homogeneous tanks, the interior of the cartridge and the chamber, which communicate through the holes in the tail after the cardboard has been pierced beyond its bursting pressure. In each of the tanks, the powder in it burns at its own speed. Each point will be detailed below separately. This approach has barely been explored. In fact, the only apparent document offering a similar work is an article by Anderson [2], the rest involving a spatial study of the problem, as proposed by Kuo [12], or to impose the behavior of the igniter. The chosen configuration is shown in figure 1.

2.1 Gas thermodynamics

The vast majority of the thermodynamic principles of this model are based on those given in the work of K. Kuo [12]. Starting from the Noble-Abel equation of state (2.1) :

$$P = \frac{r\,T}{\frac{1}{\rho} - b} \tag{2.1}$$

A certain number of results are deduced from it, like the expression of the mass internal energy (2.2) :

$$U_m = \frac{r\,T}{\gamma - 1} \tag{2.2}$$

Or the thermodynamic identity of the enthalpy :

$$dH_m = \frac{\gamma\,r}{\gamma - 1} dT + b\,dP \tag{2.3}$$

It follows from this choice of EOS that the value of γ is constant

2.2 Initial condition

The striker initiates the percussion cap, which ignites the pyrotechnic ignition composition, this will cause the combustion of a small gargoyle of powder identical to that contained in the cartridge. All this is confined using a straw which will break due to the overpressure, thus releasing the gases which will flow into the diffuser and spread into the cartridge. The rest of the powder will then ignite and burn until it reaches the bursting pressure of the cardboard. As a choice of initial condition, it starts from the bursting pressure of the cardboard and it determines the necessary mass of powder to burn to reach this state. It is then assumed that all the powder burns homogeneously until the gas reaches the bursting pressure of the cardboard. The hypothesis of a homogenous combustion is not accurate, it is however difficult to split off it here. We will keep this hypothesis in mind when comparing simulations and experiments. It remains to solve the following system (2.4), whose unknowns are T_{init} and m_{ginit}, where $init$ subscript refers to the initial value in the code :

$$\left\{\begin{array}{rl} P_{init} = & \left(\frac{m_{air}}{M_{air}} + \frac{m_{ginit}}{M_g}\right)\frac{R\ T_{init}}{V_0 - V_{gp1}} \\ T_{init} = & \frac{\Delta_r U\ m_{ginit}}{C_{Vair} m_{air} + C_V m_{ginit}} + T_0 \end{array}\right. \tag{2.4}$$

When m_{ginit} is known, the mass of remaining powder can be deduced. The combustion is assumed to be homogeneous so the thickness that burned e_b through :

$$\frac{V_{grain}(e_b)}{V_{grain}(0)} = 1 - \frac{m_{ginit}}{m_0}$$

2.3 System of conservation equations

The following system (2.5) models the gas phase in the cartridge, referenced as subscript 1, also subscript i denotes the values at the interface between the 2 chambers :

$$\left\{\begin{array}{rl} d_t m_{g1} = & \rho_p\ A_{gp1}\ V_{c1} - A\ \rho_i\ u_i \\ d_t T_1 = & \frac{\gamma-1}{m_{g1}\ r}\left(\rho_p\ A_{gp1}\ V_{c1}\ \left(\Delta_r U - \frac{r}{\gamma-1}(T_1 - T_0)\right) - P_i\ u_i\ A + P_1\ d_t V_{gp1}\right. \\ & \left. - A\ \rho_i\ u_i\ r\frac{T_i - T_1}{\gamma-1}\right) \\ \rho_1 = & \frac{m_{g1}}{V_{cartridge} - V_{gp1}} \\ P_1 = & \frac{r\ T_1}{\frac{1}{\rho_1} - b} \end{array}\right. \tag{2.5}$$

With, in order, the equation of conservation of mass, of energy, the density of gases and the Noble-Abel equation of state. The conservation equations are integrated on the gas volume of the cartridge: $m_g = \iiint_{V_{free}} \rho\ dV$ and $U = \iiint_{V_{free}} \rho\ r\ T/(\gamma - 1)\ dV$. The counterpart system for the gas in the chamber (subscript 2) can be described as follows :

$$\left\{\begin{array}{rl} d_t m_{g2} = & \rho_p\ A_{gp2}\ V_{c2} + A\ \rho_i\ u_i \\ d_t T_2 = & \frac{\gamma-1}{m_{g2}\ r}\left(\rho_p\ A_{gp2}\ V_{c2}\ \left(\Delta_r U - \frac{r}{\gamma-1}(T_2 - T_0)\right) + P_i\ u_i\ A + P_2\ d_t V_{gp2}\right. \\ & \left. - P_2\ \pi\ R_c^2\ v_{ammu} + A\ \rho_i\ u_i\ r\frac{T_i - T_2}{\gamma-1}\right) \\ \rho_2 = & \frac{m_{g2}}{V_{chamber} - V_{gp2}} \\ P_2 = & \frac{r\ T_2}{\frac{1}{\rho_2} - b} \end{array}\right. \tag{2.6}$$

The mass conservation equation is a simple balance in which is found the source term due to the combustion of the powder and the exchange term whose parameters are expressed in the following part. The energy conservation equation is an internal energy balance, the kinetic energy of gases is neglected. Indeed, the mortar ammunition

velocity goes up to $400\ m.s^{-1}$ with a speed of sound of approximately $1000\ m.s^{-1}$ for an approximately $1\ m$ long barrel. Moreover, it is legitimate to not consider the heterogeneities of pressure and the flow of gases inside the tanks.
The unknowns are the thermodynamic parameters of the two tanks. The combustion rates are functions of these quantities. The volume of the chamber is a function of the displacement of the ammunition. Finally, the values linked to the flow of gases from one tank to another are described in the following section.
In system (2.6), the possible presence of grains in the chamber is taken into account, this makes it possible to consider those which could come out of the cartridge or else those which would already be present in the case initially not envisaged where extra powder would be considered.

2.4 Flow law

The calculus starts from Anderson's idea [2]. The present situation matches a compressible flow comparable to the one in a convergent of a nozzle. However, it is not possible to start from the laws established for rockets because they are based on the use of the ideal gas law, which does not apply here. It was necessary to start from the hypothesis of homentropic flow and the expression of the enthalpy (2.3) to deduce the following law :

$$u_i = \sqrt{2\,b(P_1 - P_2) + 2\frac{\gamma}{\gamma-1}\frac{P_1}{\rho_1}\frac{1}{1-b\,\rho_1}\left(1-\left(\frac{P_2}{P_1}\right)^{\frac{\gamma-1}{\gamma}}\right)(1-b\,\rho_1)^2} \tag{2.7}$$

This law (2.7) is valid when $P_1 > P_2$ but within a certain limit, the flow cannot be supersonic because there is only a convergent. There is therefore a limit speed that can be determined by first solving the following equation :

$$\begin{aligned}\frac{\gamma}{\gamma-1}P_1\left(\frac{1}{\rho_1}-b\right)+b\,P_1 =& \frac{\gamma}{\gamma-1}P_{lim}\left(\frac{1}{\rho}-b\right)\left(\frac{P_1}{P_{lim}}\right)^{\frac{1}{\gamma}}+b\,P_{lim}\\ &+\frac{\gamma}{2}P_{lim}\left(b+\left(\frac{1}{\rho_1}-b\right)\left(\frac{P_1}{P_{lim}}\right)^{\frac{1}{\gamma}}\right)^2\left(\frac{1}{\rho_1}-b\right)^{-1}\left(\frac{P_{lim}}{P_1}\right)^{\frac{1}{\gamma}}\end{aligned}$$

If $P_2 > P_{lim}$ then the law (2.7) given previously is valid and $P_i = P_2$, otherwise the flow will be sonic :

$$u_i = \sqrt{\gamma\frac{P_{lim}}{\rho_{lim}(1-b\,\rho_{lim})}} \tag{2.8}$$

With $P_i = P_{lim}$ and $\rho_{lim} = \left(b+\left(\frac{1}{\rho_1}-b\right)\left(\frac{P_1}{P_{lim}}\right)^{\frac{1}{\gamma}}\right)^{-1}$.
It remains to determine the temperature and the density of the gases, which is determined via :

$$\rho_i = \frac{1}{b+\left(\frac{1}{\rho_1}-b\right)\left(\frac{P_1}{P_i}\right)^{\frac{1}{\gamma}}}$$

$$T_i = \frac{P_i}{r}\left(\frac{1}{\rho_1}-b\right)\left(\frac{P_1}{P_i}\right)^{\frac{1}{\gamma}}$$

All this calculus were derived considering a flow coming from the cartridge toward the chamber. However the same can be done in the reverse direction, i.e. $P_2 > P_1$.

2.5 Grain transport modeling

Powder could come out of the cartridge. If the grains are small compared to the size of the holes and they have the same speed as the flow, then the same law as Kuo [13] can be used :

$$D_{m\ powder} = \frac{\alpha_2}{1-\alpha_2} D_m$$

With α_2 the mass fraction of solid. These hypotheses are not valid here and this law gives a too high grain flow, a solution is to put a corrective factor there which is worth approximately $0,1$. This approach is similar to what Anderson [2] gives the following equation (2.9) :

$$D_{m\ powder} = \frac{\alpha_2}{1-\alpha_2} D_m\ f_{tr} \tag{2.9}$$

With $f_{tr} = u_p/u_i$.
An inertial frictional force is considered, then one can deduce a characteristic time for a grain to get to the speed of the flow :

$$\tau = \frac{2\ m_{grain}}{\rho\ u_i\ C_x\ A_{grain}} \approx 1\ ms$$

Therefore the grains cannot be considered immobile nor at the same speed as the flow because it is of the same order of magnitude as the duration of the equilibrium of the chambers. Then a transport velocity of the grains can be determined and assume that they are set in motion to leave the cartridge without returning. Knowing that once the flow velocity is reached, it is assumed that $f_{tr} = 1$.
In Nussbaum's thesis [14], he refers to an article to describe powder entrainment[15, 16] that refer to Burke [17]. Our goal is to determine a frictional force which applies to a grain.

$$F = \frac{1-\alpha_2}{d_V N_{gp}} \frac{\Delta P}{L}$$

Then one can use Ergun's law [16] :

$$\frac{\Delta P}{L} g = \frac{150}{g} \left(\frac{\alpha_2}{1-\alpha_2} \right)^2 \frac{\mu\ u_i}{D^2} + \frac{1,75}{g} \frac{\alpha_2}{1-\alpha_2} \frac{\rho\ u_i^2}{D}$$

With $D = \frac{6\ V_{grain}}{A_{grain}}$ and $d_V\ N_{gp} = \frac{\alpha_2}{V_{grain}}$ the result is :

$$F = \frac{A_{grain}}{6} \left(\frac{150}{g} \frac{\alpha_2}{1-\alpha_2} \frac{\mu\ u_i}{D} + \frac{1,75}{g} \rho\ u_i^2 \right)$$

Thus :

$$\partial_t u_p = \frac{A_p}{6\ \rho_p\ V_{grain}} \left(k_1 \frac{\alpha_2}{1-\alpha_2} \frac{\mu\ (u_i - u_p)}{D} + k_2 \rho\ (u_i - u_p) |u_i - u_p| \right)$$

The flow is in turbulent regime so the viscous term is negligible and obtain the following equation :

$$\partial_t u_p = \frac{k_2}{D\ \rho_p} \rho\ (u_i - u_p) |u_i - u_p| \tag{2.10}$$

Which is almost equivalent to an inertial frictional force in the case of a sphere with the given value of k_2 :

$$\rho_p\ V_{grain}\ \partial_t u_p = \frac{4\ k_2}{3} \frac{1}{2}\ S\ \rho\ u_i^2$$

The values of the coefficients being dependent on the original units used by the authors, the value of k_2 can be deduced from the value of C_x of a sphere: $k_2 = 3/4\ C_x \approx 0,37$ instead of 0.18. The authors seem to mean that this coefficient is dependent on the shape of the grain.
This law was improved by Harrison [18]. Tallmadge proposed an improvement [19] which specifies Ergun's inertial correlation. They give equivalent values of $k_2 \approx 4.5$

$$\partial_t u_p = \frac{A_p}{6\ \rho_p\ V_{grain}} \left(k_1 \frac{\alpha_2}{1-\alpha_2} \frac{\mu\ (u_i - u_p)}{D} + k_2 \left(\frac{\alpha_2}{1-\alpha_2} \frac{\mu}{\rho\ u_i\ D} \right)^{1/6} \rho\ (u_i - u_p)|u_i - u_p| \right)$$

Which is supposed to work up to $\mathcal{R}_e = 10^5$. Once again, the viscous part is neglected to finally obtain :

$$\partial_t u_p = \frac{k_2\ D}{\rho_p} \rho \left(\frac{\alpha_2}{1-\alpha_2} \frac{\mu}{\rho\ u_i\ D} \right)^{1/6} (u_i - u_p)|u_i - u_p| \tag{2.11}$$

The value of k_2 in the equation (2.11) is to be specified because it is valid for the flow of near-spherical grains in a cylinder, here the shape of the cartridge makes the flow more difficult.

2.6 Generalized Vieille's law

In solid combustion, Vieille's empirical law $V_c = a_v\ P^n + b_v$, where a_v, b_v and n are assumed constant values. It is often used ans is well documented so we will not go into detail here. It can be applied subject to sufficiently weak flow at the level of the surface of the solid, otherwise erosion phenomena may appear.
This empirical law operates on given pressure ranges when the seed is ignited, so ignition phenomena cannot be taken into account.
To explain this theoretically too slow combustion, the following model has been found.

2.7 Erosive burning

There are many reliable relationships to model erosive combustion. One of the simplest [20], but accurate for double base, is chosen.

$$\epsilon = \begin{cases} 1 & \text{if } Vi < 8 \\ 1 + 0,05\ (Vi - 8) & \text{otherwise} \end{cases} \tag{2.12}$$

$$Vi = \frac{\rho_g\ U}{\rho_s\ r} \sqrt{\xi}$$

$$\xi = 0,0032 + \frac{0,22}{Re^{0,237}}$$

In our case : $Re \approx 2.10^6$, $\rho_g \approx 50\ kg.m^{-3}$, $\rho_s \approx 1600\ kg.m^{-3}$, $U \approx 1000\ m.s^{-1}$, $r \approx 0,1\ m.s^{-1}$, $\epsilon \approx 2$, this was expected. This reinforces the validity of the presence of erosive combustion.

3 POLYDISPERSE GUNPOWDER SIZE

3.1 Simple geometry

It is mandatory to determine the surface area and volume of the grain over time. The variable z representing the mass fraction of burnt powder is usually used to express geometric quantities, here we have chosen to take a different variable: e_b to simplify the digital task. So they are going to be expressed as a function of the thickness

that has burned up to a time T, which is determined via :

$$e_b(T) = \int_0^T V_c(t)\, dt$$

This gives for the flakes, which are rectangular parallelepipeds with one side square, of thickness d and of length l :

$$A_{grain} = 4(d - 2\, e_b)(l - 2\, e_b) + 2(l - 2\, e_b)^2$$

$$V_{grain} = (d - 2\, e_b)(l - 2\, e_b)^2$$

3.2 Gunpowder size distribution

It would be naive to think that the grains of powder are all identical down to the molecular size. Then the question arises of the size limit below which all the grains can be considered as perfectly identical. There are a lot of references on the PBE[6], with practical applications in combustion [21], but very few in application to interior ballistics [7]. Considering the observed phenomena do not seem to be affected by the instabilities whose characteristic time is less than $500\ \mu s$, the combustion rate is of the order of $1\ /\ 10\ cm.s^{-1}$, then a characteristic thickness can be deduce below which there will not have an impact : $\approx 10^{-5}\ m$. However, the powders have standard deviations on the geometric parameters which are always greater than $10^{-4}\ m$, it must then be taken into account in our model. The example of the thickness of flakes will be detailed afterwards.

3.3 Distribution characterization

As a first approximation, a centered normal law reduced can be chosen, the other dimensions are assumed to be exact. Then the distribution function of the initial grain thickness is defined as follows :

$$\int_e^{+\infty} f(x)\, dx = \frac{N_{grain}(d \geq e)}{N_T} \tag{3.1}$$

This result is incompatible with a reduced centered normal distribution. However, in view of our practical case, it will be necessary to numerically calculate the integrals which result from it, we will then make the following approximation :

$$\int_0^{+\infty} f(x)\, dx \approx \int_{\bar{d}-3\sigma}^{\bar{d}+3\sigma} f(x)\, dx \approx 1 \tag{3.2}$$

This allows an abuse by considering the normal law that one wishes provided that $\bar{d} - 3\sigma \gg 0$, in the sense that one has the following inequality with a given f :

$$Int_{error} = \int_0^{\bar{d}-3\sigma} f(x)\, dx + \int_{\bar{d}+3\sigma}^{+\infty} f(x)\, dx \ll 1$$

The semantic consequence is to ignore grains whose thickness deviates by more than 3 standard deviations. A possible improvement would be to make the following calculations with a faithful distribution which may have to be determined one day without this approximation despite its legitimacy. This is verified in the case of a Gaussian distribution :

$$f(x) = \frac{e^{-\left(\frac{x-\bar{d}}{\sqrt{2}\sigma}\right)^2}}{\sqrt{2\,\pi}\sigma}$$

It gives a value of $Int_{erreur} \approx 0,27\%$. In order to correct this error, it is possible to multiply f by $1/0.9973$ to keep the value of the integral at 1.

3.4 Modification of the interior ballistics model

In our model, it is assumed that every grain is perfectly identical, which results in the presence of amounts such as the number of grains times the volume of a grain at a time t. All these dependencies can be replaced in a fairly simple way by the procedure which follows.
Let us first determine the total number of grains, by construction of f :

$$\int_{e}^{e+\delta e} f(x)\, dx = \frac{N_{grain}(e+\delta e \geq d \geq e)}{N_T}$$

Thus :

$$V_T = \Sigma N_{grain}(e+\delta e \geq d \geq e) V(e+\delta e/2) = N_T \int_0^{+\infty} f(x)\, V_{grain}(x)\, dx$$

$$N_T = \frac{m_p}{\rho_p \int_0^{+\infty} f(x)\, V(x)\, dx} \tag{3.3}$$

It simply follows that the number of grains can be deduced from the ratio of the total volume to the average volume. In the case of flakes, the dispersion of which is only studied according to the thickness, this gives a first pleasant result. :

$$N_T = \frac{V_T}{l^2 \times \bar{d}}$$

This implies that the number of grains does not change if all the grains are identical.
This first digression makes it possible to understand the changes that will be made to the model: the volumes and surfaces of grains will no longer be calculated as $N_T \times V(e_b)$ but as follows :

$$G(e_b) = N_T \int_{eb}^{+\infty} f(x) g(x, e_b)\, dx$$

Because :

$$g(x, e_b) = \begin{cases} g(x, e_b) & \text{if } x \geq e_b \\ 0 & \text{otherwise} \end{cases} \tag{3.4}$$

This is quite consistent with the ideal case of identical grains, it is enough to substitute f by a dirac centered in $\bar{d}$ to check it :

$$G(e_b) = \begin{cases} N_T\, g(\bar{d}, e_b) & \text{if } e_b < \bar{d} \\ 0 & \text{otherwise} \end{cases}$$

3.5 Digital distribution

The case of a Gaussian distribution was presented above. However, the distribution could be unspecified, such as black powder which is usually made up of potato-shaped grain with a very wide non-Gaussian distribution. Generally, it is a partition function of the volume according to the diameter which is measured, it will be therefore necessary to take care to make the conversion into number distribution. The goal being to find the surface of a fictitious grain which, once multiplied by the number of grain, will give the actual evolution of the surface over time. This method makes it possible to ignore the progressive disappearance of the grains since it is hidden in the behavior of the fictitious grain.
This gives the following result for any distribution of spherical grains:

$$S_T(e_b) = \begin{cases} N_T \int_{d_i}^{d_s} f(x)\pi(x - 2\, eb)^2\, dx & \text{if } e_b \leq d_i/2 \\ N_T \int_{2e_b}^{d_s} f(x)\pi(x - 2\, eb)^2\, dx & \text{if } d_i/2 \geq e_b \geq d_s/2 \\ 0 & \text{otherwise} \end{cases} \tag{3.5}$$

Where d_i and d_s represent respectively the minimum and maximum diameter measured. N_T can be calculated very easily since $\bar{V}_{grain}(0) = \int_{d_i}^{d_s} f(x)V_{grain}(x,0)\ dx$ represents the average volume in number so $N_T = V_{powder}/\bar{V}_{grain}(0)$.

3.6 Generic Application

The calculation of integral (3.5) is numerically expensive. A less greedy method, which furthermore allows to easily include arbitrary distributions would be to generate a table of the surface and the volume according to the reacted thickness. The gain is to be able to increase the numerical resolution. Indeed, for a Gaussian distribution, it is not necessary to have a high spatial resolution but this observation does not generalize to all distributions. An example would be aluminum [22] whose diameters can be spread over two orders of magnitude. Computing the integral at each time step would significantly increase computation times. Thenceforth, the table method will be used.

4 Example of 140mm mortar

4.1 Configuration

The geometry of a 140mm mortar is presented in Figure 1. It considers the case at the minimum load i.e. when there is only powder in the cartridge. The walls in black are interfaces which break at 100 atm. The ammunition mass has been fixed at 20 kg.

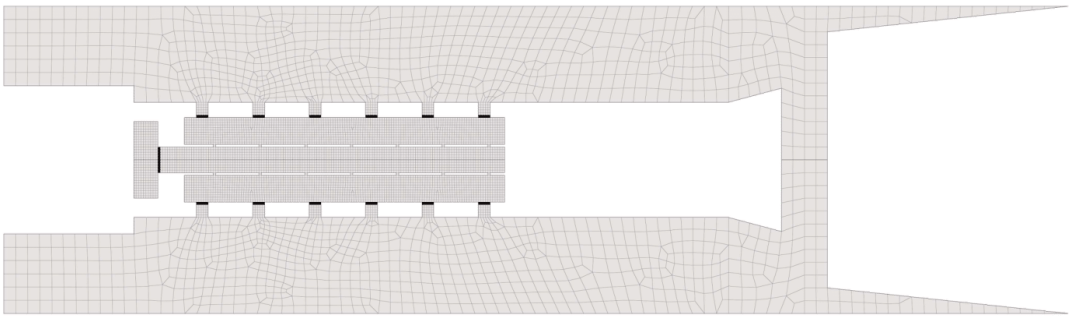

Figure 1: 2D mesh

The chosen powder will be a 3x3x0,3 double base. The dispersion of grain thickness is set to 20%. This gives the modification of the surface that can be observed in Figure 2. The length of the course is taken at 1 m.

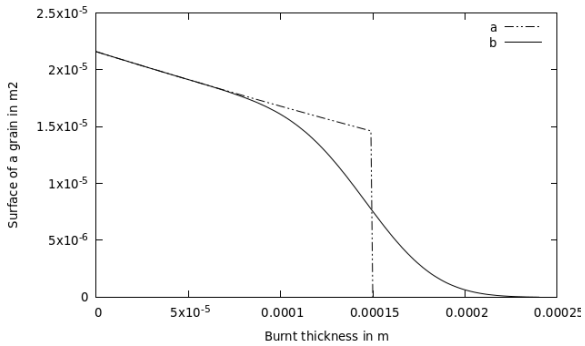

Figure 2: a) Surface of the average grain, b) Average surface considering the distribution

4.2 Results

To compare MOBIDIC and SBIM, one needs to determine the average pressure in the chamber which is calculated via $\bar{P}_{chamber}(t) = \iint_{chamber} P(t,x,y)\ 2\pi\ y\ dxdy / \iint_{chamber} 2\pi\ y\ dxdy$. The results are trustworthy given the proximity of the predictions between the two codes in the figures 3 and 4.

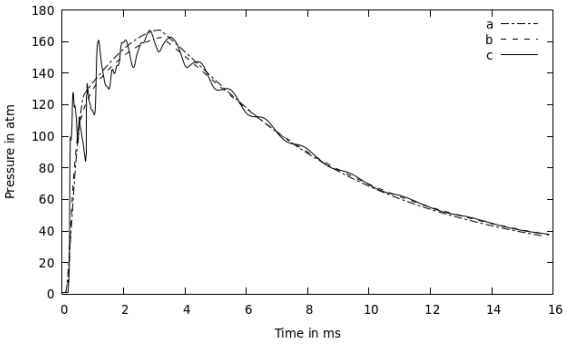

Figure 3: a) SBIM average pressure in the mortar's chamber, b) MOBIDIC average pressure in the mortar's chamber, c) MOBIDIC pressure sensor in the mortar's chamber

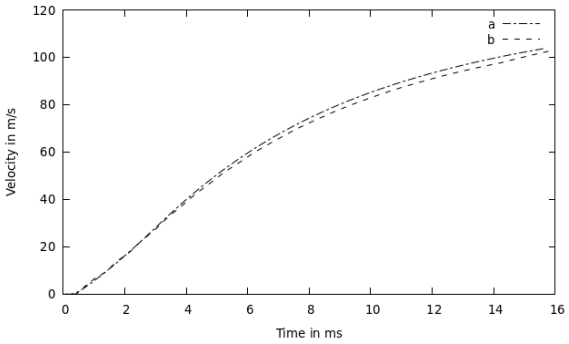

Figure 4: Ammunition velocity over time a) SBIM, b) MOBIDIC

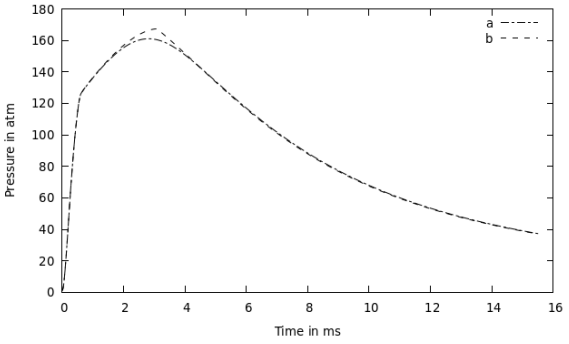

Figure 5: a) SBIM average pressure in the mortar's chamber, b) SBIM average pressure in the mortar's chamber with polydisperse size

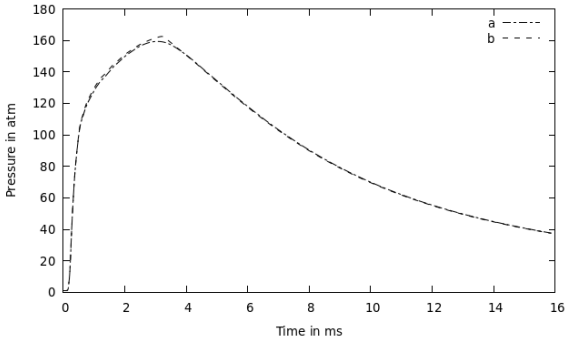

Figure 6: a) MOBIDIC average pressure in the mortar's chamber, b) MOBIDIC average pressure in the mortar's chamber with polydisperse size

Code	no dispersion	with dispersion
MOBIDIC	$102,74\ m.s^{-1}$	$102,69\ m.s^{-1}$
SBIM	$103,67\ m.s^{-1}$	$103,51\ m.s^{-1}$

Table 1: Final velocity

Code	no dispersion	with dispersion
MOBIDIC	$162,52\ atm$	$159,33\ atm$
SBIM	$167,3\ atm$	$161,0\ atm$

Table 2: Maximum pressure reached

5 CONCLUSION

One can note a good agreement between SBIM and MOBIDIC. The addition of the dispersion makes it possible to correct the breaks in slope on the pressure curves which are not observed experimentally. Also, the presence of this dispersion can be favorable. Indeed, the maximum pressure is reduced but the exit velocity is almost unchanged. An interesting problem to study would be the case of a configuration where the powder finished burning at the end of the simulation, the dispersion of the grains could deduce an end of combustion after the ammunition exits contrary to the model of the ideal grain.

References

[1] Ragini Acharya et al. *Comprehensive Modeling and Numerical Simulation of Interior Ballistic Processes in 120mm Mortar With Systematic Experimental Validation.* PENNSYLVANIA STATE UNIV UNIVERSITY PARK, Dec. 1, 2008.

[2] Ronald D. Anderson. *IBHVG2: Mortar Simulation With Interior Propellant Canister.* ARMY RESEARCH LAB ABERDEEN PROVING GROUND MD, 2006.

[3] Ruihua Zhang et al. "Study on dynamic burning rate equation of propellant". In: *Propellants, Explosives, Pyrotechnics* 42.6 (2017).

[4] H. S. Mukunda and P. J. Paul. "Universal behaviour in erosive burning of solid propellants". In: *Combustion and Flame* 109.1 (Apr. 1997).

[5] V. Arkhipov et al. "Solid propellant combustion in a high-velocity cross-flow of gases (review)". In: *Combustion, Explosion, and Shock Waves* 52 (Sept. 1, 2016).

[6] S. Rigopoulos. "Population balance modelling of polydispersed particles in reactive flows". In: *Progress in Energy and Combustion Science* 36.4 (Aug. 1, 2010).

[7] D. F. Aldis and D. Gidaspow. "Combustion of a polydispersed solid using a particle population balance". In: *Powder Technology* 57.4 (Apr. 1, 1989).

[8] R. Trębiński and M. Czyżewska. "An Approximate Model for the Theoretical Prediction of the Velocity Increase in the Intermediate Ballistics Period". In: *Central European Journal of Energetic Materials* (Vol. 12, no. 1 2015).

[9] G. Monreal-González et al. "One-Dimensional Modelling of Internal Ballistics". In: *Journal of Energetic Materials* 35.4 (Oct. 2, 2017).

[10] Ardeshir Bangian Tabrizi, Mehrzad Shams, and Reza Ebrahimi. "Numerical study of gas-solid reactive flow in a cylinder". In: *Journal of mechanical science and technology* 26.3 (2012).

[11] P. Della Pieta and C. Reynard. "Numerical investigation for modeling interior ballistics two-phase flow". In: *Proceedings of the European Forum on Ballistics of Projectiles.* 2000.

[12] Ragini Acharya and Kenneth K. Kuo. "Finite element simulation of interior ballistic processes in 120-mm mortar system". In: *Proc. of the 23rd International Symposium on Ballistics (Tarragona, Spain, 16-20 April 2007).* Vol. 1. Citeseer, 2007.

[13] Peter J. Ferrara and Jeffrey D. Moore. "Method of characteristics simulation of interior ballistic processes of M1020 ignition cartridgein A 120-mm mortar system". In: *International Journal of Energetic Materials and Chemical Propulsion* 6.5 (2007).

[14] Julien Nussbaum. "Modélisation et simulation numérique d'un écoulement diphasique de la balistique intérieure". PhD thesis. Université Louis Pasteur - Strasbourg I, Nov. 27, 2007.

[15] S. Ergun and A. Orning. "Fluid Flow through Randomly Packed Columns and Fluidized Beds". In: (1949).

[16] Sabri Ergun. "Fluid flow through packed columns". In: *Chem. Eng. Prog.* 48 (1952).

[17] S. Pt Burke and W. B. Plummer. "Gas flow through packed columns1". In: *Industrial & Engineering Chemistry* 20.11 (1928).

[18] Luke D. Harrison, Kyle M. Brunner, and William C. Hecker. "A Combined Packed-Bed Friction Factor Equation: Extension to Higher Reynolds Number with Wall Effects". In: *AIChE Journal* 3.59 (2013).

[19] J. A. Tallmadge. "Packed bed pressure drop—an extension to higher Reynolds numbers". In: *AIChE Journal* 16.6 (1970).

[20] V. Arkhipov et al. "Solid propellant combustion in a high-velocity cross-flow of gases (review)". In: *Combustion, Explosion, and Shock Waves* 52 (Sept. 1, 2016).

[21] D. B. Spalding. "The SHADOW method of particle-size calculation in two-phase combustion. 19th Symp.(Int) on Combustion". In: *The Combustion Institute, Pittsburgh* (1982).

[22] I. A. Semenov and B. V. Matsevich. "Dynamic Features of Combustion of Polydisperse Aluminum Powders in a Gas". In: *Combustion, Explosion and Shock Waves* 41.4 (July 1, 2005).